JACS Au
AN OPEN ACCESS JOURNAL OF THE AMERICAN CHEMICAL SOCIETY

pubs.acs.org/jacsau

Article

Mapping Out the Nonconjugated Organic Radical Conductors via Chemical or Physical Pathways

Jaehyoung Ko, Ilhwan Yu, Seung-Yeol Jeon, Daewon Sohn, Sung Gap Im, and Yongho Joo*

Cite This: *JACS Au* 2022, 2, 2089–2097

Read Online

ACCESS | Metrics & More | Article Recommendations | Supporting Information

ABSTRACT: Stable, nitroxide-based organic radicals have gained tremendous attention in a wide range of research fields, ranging from solid-state electronics to energy storage devices. While the success of these organics has been their designer flexibility and the processability that can fully potentiate the open-shell chemistry, a significant knowledge gap exists on the solid-state electronics of small-molecular radicals. Herein, we examine the structure–property relationship that governs the solid-state electronics of a model nitroxide and its derivatives by seeking the connection to their well-established, electrolyte-based chemistry. Further, we propose a general strategy of enhancing their solid-state conductivity by systematic humidity control. This study demonstrates an open-shell platform of the device operation and underlying principles thereof, which can potentially be applied in a number of future radical-based electronic devices.

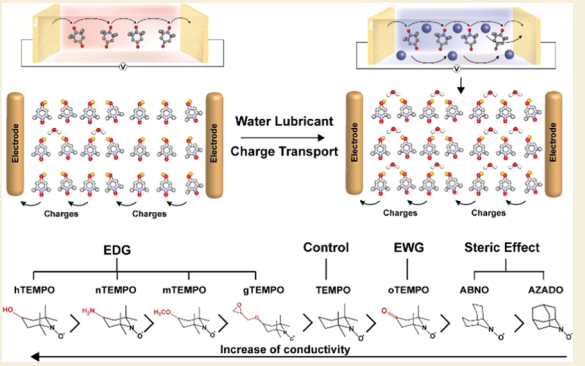

KEYWORDS: *nonconjugated conductor, open-shell chemistry, organic radicals, solid-state conductivity, electrocatalytic activity*

INTRODUCTION

Organic radicals, in which small- or macromolecules bearing stable open-shell units transport charges both electronically and ionically, have emerged as extremely useful active materials for various future device applications, including solid-state electronics,[1−10] energy storage,[10−18] and electrocatalysis.[19−22] Key advantages of these charge-neutral, nonconjugated (macro)molecules compared to the conventional, conjugated ones are (1) the structural flexibility that benefits the ultimate material processing owing to their nonconjugated nature, (2) the relatively higher degree of freedom in the molecular design to achieve the desired structure–property relationship, and (3) the high electrical conductivity without any chemical doping strategy that may negatively affect the stability and longevity of the devices.[1,23]

Among various organic radicals reported so far, stable nitroxide-based radicals, typified by (2,2,6,6-tetramethylpiperidin-1-yl)oxyl (TEMPO) and its derivatives, have been of the most intensive research focus mainly due to their excellent stability and fast exchange kinetics.[17] While these radicals have conventionally been utilized in the form of both small- and macromolecules in various wet chemistries (or electrolyte-based systems), a recent breakthrough in a solid-state conductivity of a macromolecular TEMPO has brought about a dramatic increase in research interests on the solid-state electronics of such organic radicals.[1,23] As such, various TEMPO-based radical polymers have been revisited since then in terms of their solid-state electronics.[23−27]

Small-molecular TEMPO and the derivatives, on the other hand, also present a key significance in the solid-state electronics of organic radicals. The main advantage of such radicals compared to the macromolecular ones is their high radical density owing to the absence of insulating backbone structures, which is beneficial to the electronic performance of the resultant devices. Also, as has been found in conjugated organics, fundamentals established on small-molecular radicals are expected to be readily translated into the designer macromolecular radicals, which altogether will realize high-performance radical electronics in the near future.[23,28] Thus, it is of key importance that one establishes a comprehensive understanding of these small-molecular radicals and the context they are in, among relevant subfields of open-shell chemistry.

The missing gap in the understanding of the small-molecular TEMPOs in solid-state electronics, however, has mainly been due to the difficulty in measuring their electronic properties, owing to their characteristic physical properties. In a previous paper, we first reported that the solid-state conductivity of a TEMPO derivative in its molten state can indeed be measured

Received: June 20, 2022
Revised: July 21, 2022
Accepted: July 27, 2022
Published: August 26, 2022

https://doi.org/10.1021/jacsau.2c00361
JACS Au 2022, 2, 2089–2097

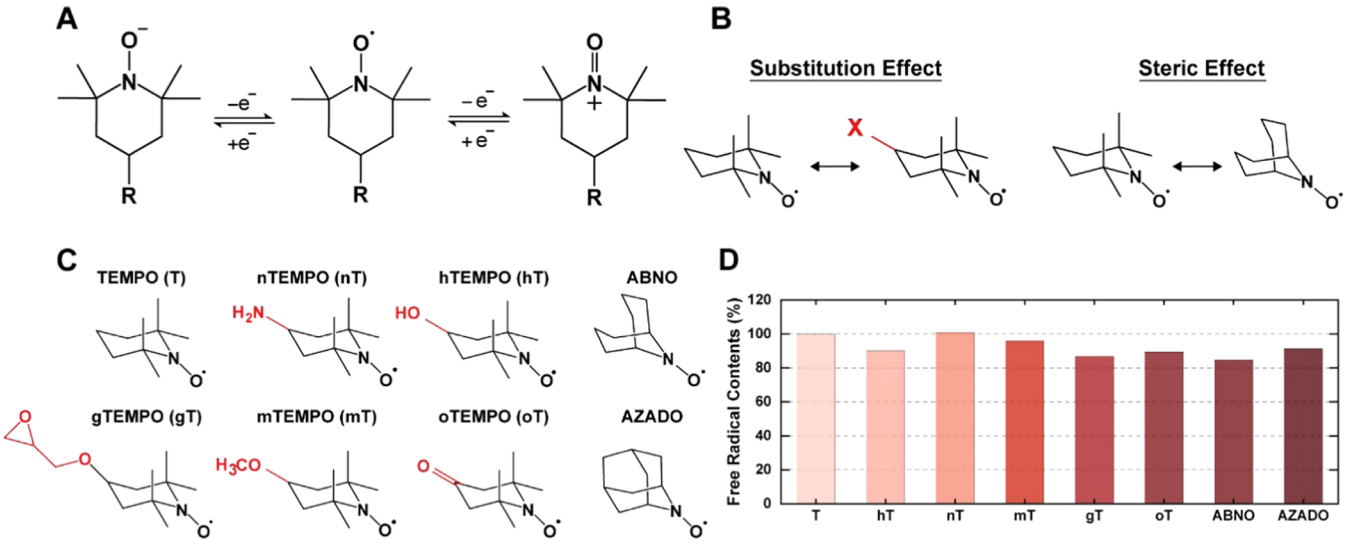

Figure 1. Chemistry of nitroxide-based small-molecular radicals. (A) Self-exchange redox reaction of TEMPO derivatives and (B) possible effects on the electronic properties of TEMPO derivatives. (C) Chemical structure of TEMPO derivatives in this study, and (D) radical density of each compound.

and is comparable to that of highly conducting macromolecular TEMPOs.[23] Further, we developed this idea into electronically and ionically doping the small-molecular radical, achieving a solid-state conductivity that exceeds that of the doped macromolecular radicals.[29] Building upon the understanding of the conduction behavior found in the small-molecular TEMPO, here we expand the measurement of the solid-state conductivities of a series of TEMPO derivatives and compare the observed structure−property relationship with the electrocatalytic trends reported in wet systems, thereby connecting the two intensive fields of research.

In an attempt to achieve higher room-temperature solid-state conductivity of small-molecular TEMPO derivatives, it was found that their crystal structures minimizing the steric hindrance act as the major hindrance toward efficient electron transfer.[23] Thus, we hypothesized that an appropriate physical modification of the packing structure should affect their electronic behavior significantly, by breaking the symmetry and modulating the proximity between the active radical sites. Motivated by the role of water as a plasticizer in a number of organic films, we apply a systematic variation of the relative humidity of the system, thereby achieving a reversible modulation of the solid-state conductivity of the TEMPO derivatives. Further, we develop this idea into proof-of-concept TEMPO devices and their utilization as humidity sensors. We believe our study on the structure−property relationship of the open-shell chemistry and its expansion toward a more generalizable concept of conductivity modulation will serve as a platform for future applications of open-shell organics, including organic electronics, electrocatalysts, and energy storage systems.

RESULTS AND DISCUSSION

Small-molecular organic radicals utilized in this effort, which are designed to demonstrate the structure−property relationship of nitroxide-based radicals in the solid state, include TEMPO and its derivatives. Upon their electronic conduction, single-electron transfer from the valence shell leads to a fast intermolecular charge transport without breaking of the chemical bond.[30] Specifically, these chemical species undergo a redox reaction by switching between chemical structures, from a neutral radical to an oxoammonium cation, or to an aminoxyl anion (Figure 1A).[31] The redox reaction occurs in both the wet and the dry system, although the mechanisms by which electrons are transferred differ between the two.[30] While a series of redox reactions on the active radical sites lead to charge transfer in the wet system, an electric-field-driven intermolecular electron hopping adds up to the overall conduction mechanism in the solid state.[10,30] In both cases, the designing architecture of the molecules plays an important role in optimizing the properties of the materials for the desired performance of the device operation.[19]

In general, the electronic band structure of organic (semi)conductors is engineered through the modular design of molecular components.[32] In open-shell chemistry, a similar strategy can be utilized, such that a specific functionality placed near the stable radical affects the molecular electronic structure. While the substitution effect may not be as effective as typical pi-conjugated organics owing to the nonconjugated nature of the radical species, the previous theoretical approach has revealed significant modulation of the electronic structure of TEMPO-based molecules, following chemical modification in the 4′ position of the TEMPO ring.[19] Further, the steric effect placed near the active radical site of TEMPO has been shown to dramatically impact the catalytic activity of resultant TEMPO derivatives, which seems rather unexpected when judged from the observed redox potential trend of these molecules.[21] As such, we group different types of TEMPO derivatives into two and explore the impact of functionality variation on solid-state electronic conductivity (Figure 1B).

The first group of interest includes TEMPO (T), 4-hydroxy TEMPO (hT), 4-amino TEMPO (nT), 4-glycidyloxy TEMPO (gT), 4-methoxy TEMPO (mT), and 4-oxo TEMPO (oT) (Figure 1C). The series are designed such that there exists a significant difference in the effect of electron-donating or -withdrawing functionality on the active radical site. An additional subcategorization within the first group was conceived, where the TEMPO derivatives with hydroxyl and amino groups (hT and nT) are expected to exhibit characteristic phase behavior, in addition to the electron-

https://doi.org/10.1021/jacsau.2c00361
JACS Au 2022, 2, 2089−2097

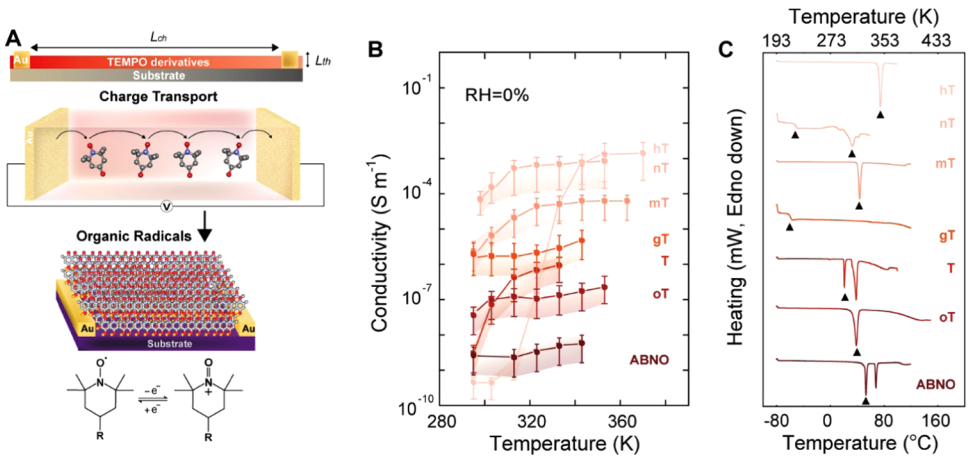

Figure 2. Solid-state electronics based on TEMPO derivatives. (A) Schematic illustration of TEMPO-based devices with a channel length of 50 μm and film thickness of 90 μm. (B) Temperature-dependent conductivity of TEMPO derivatives. (C) DSC thermograms of selected TEMPO derivatives.

donating effect that the two functionalities provide owing to the presence of the hydrogen-bonded network (*vide infra*).[28] The second group under investigation includes sterically less hindered nitroxides that have frequently been utilized in the wet chemistry of TEMPO derivatives for alcohol oxidation,[19,21] and it includes 2-azaadamantane *N*-oxyl (AZADO) and 9-azabicyclo[3.3.1]nonane-*N*-oxyl (ABNO) (Figure 1C). Taking advantage of the small-molecular nature, all of the radicals featured a high radical content as compared to the pristine T as an external standard, based on electron spin resonance (ESR) calculation on each TEMPO derivative (Figure 1D, and Figures S2–S9).

Temperature-Dependent Conductivity of TEMPO Derivatives

We first measured the electrical conductivity of the TEMPO derivatives as a function of temperature in a vacuum (Figure 2A). Briefly, on top of a glass substrate, Cr/Au electrodes (10/50 nm) were deposited for the current–voltage sweep, with a measurement unit equipped with a temperature controller. After the deposition of the electrodes, TEMPO derivatives were placed in a PDMS mold that leaves room for a connecting channel between the two electrodes, into which a solution of each TEMPO was drop-cast and dried. Conductivity values were then calculated considering the geometric parameters of the resulting channel (detailed information on conductivity measurement is described in the Experimental Section). In our previous report, we described a temperature-dependent conductivity of hT, where a dramatic change in the apparent conductivity was observed following a phase transition of hT from a crystalline phase to a molten solid phase.[23] Specifically, hT featured very low conductivity (10^{-9}–10^{-10} S m^{-1}) at room temperature owing to its crystalline nature. In sharp contrast, the hT at a high temperature close to its melting point (T_m) displayed a very high conductivity of 10^{-2}–10^{-3} S m^{-1}, showing a difference of >10^5 S m^{-1} between the two temperatures. Here, we describe the physical state of TEMPO derivatives as being a "thermally activated" state when significantly above room temperature but below T_m. It is thought to provide a fast transport of charges by allowing increased thermal motion of the molecules, which facilitates self-exchange redox reaction and/or electron hopping between active radical sites.

Systematic measurements on the temperature-dependent conductivity of TEMPO derivatives indicated that the observed temperature dependence of hT is a general trend of small-molecular TEMPOs that are crystalline at room temperature (Figure 2B). For example, we found that the TEMPO derivatives having a distinct melting point (nT, mT, T, oT) show a similar temperature dependence as that of hT (Figure 2C). Specifically, we found that the molten solid of each TEMPO derivative exhibits significantly higher conductivity than that at room temperature, for nT (~305 K), mT (~315 K), T (~310 K), and oT (~310 K). On the other hand, gT, which features no distinct T_m, only showed a thermally activated insulating behavior, as per its rubbery state above the glass-transition temperature (T_g) within the conductivity measurement window. Notably, T_g appeared in gT due to the presence of the epoxy group, which minimizes the crystal nature of the organic radical. The apparent solid-state conductivity and the conductivity difference between the low and the high temperatures (which we refer to as a thermal on/off ratio, in a nonrigorous and descriptive way) were strongly dependent on the nature of functionality appended to the TEMPO ring. For example, the observed conductivity of oT (10^{-7} S m^{-1}) featuring a ketone at the 4′ position showed a sharp contrast to that of hT (10^{-3} S m^{-1}) at 310 K. Overall, the measured conductivity values at their thermally activated state followed the trend of hT> nT> mT> gT> TEMPO> oT> ABNO. The observed thermal on/off ratios were ~10^7 for hT, ~10 for nT, ~10 for mT, ~5 for oT, ~10^2 for TEMPO, and ~10 for ABNO at relevant temperature ranges. Interestingly, however, the conductivity of the sterically less hindered TEMPO (ABNO) showed the one that is the lowest among all of the observed TEMPO derivatives despite its distinct T_m that is comparable to those of nT and hT. Specifically, we found again a simple, thermally activated insulating behavior from it without any abrupt increase in conductivity. While the origin of this behavior is currently unclear, we believe it is closely related to the short lifetime of free radicals that the sterically less hindered TEMPO derivatives feature. It indicates that radical stability, along with the nature of the functionality, plays an important role in determining the total conductivity of the radical molecules.

https://doi.org/10.1021/jacsau.2c00361
JACS Au 2022, 2, 2089–2097

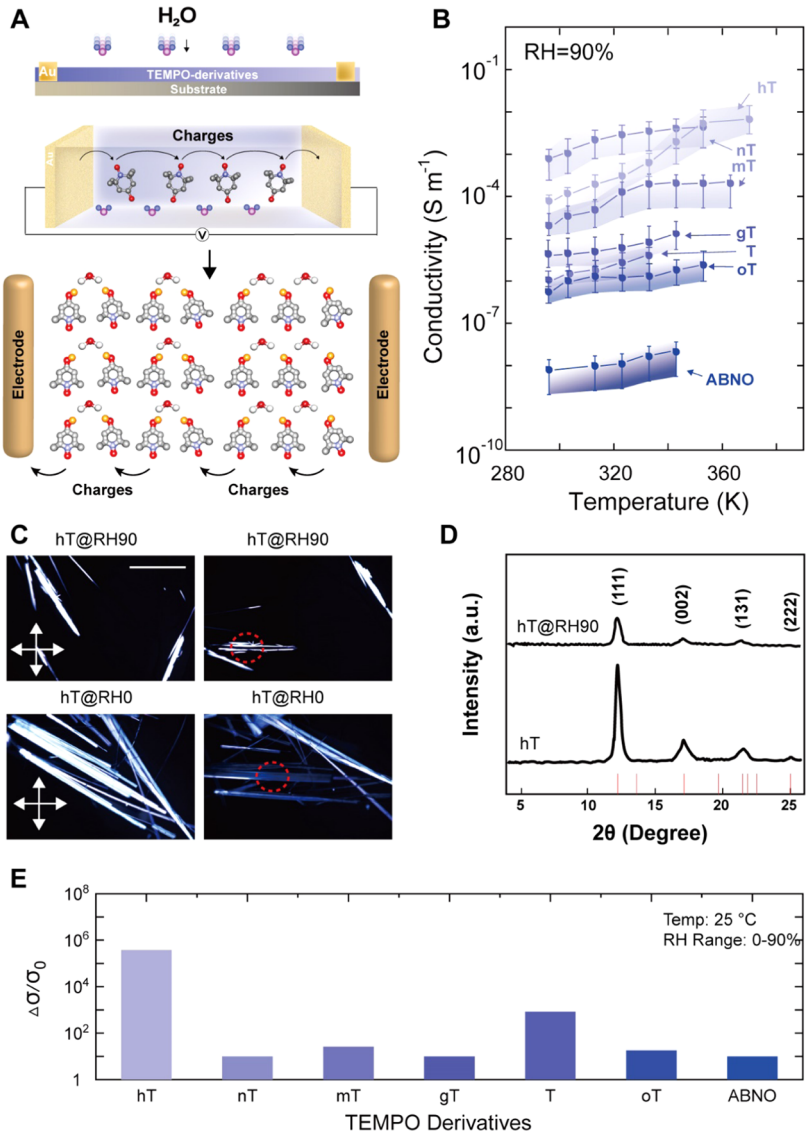

Figure 3. Effect of humidity on the solid-state conductivity of selected TEMPO derivatives. (A) Schematic illustration of the TEMPO-based device under a wet environment. (B) Temperature-dependent conductivity of TEMPO derivatives at RH = 90%. (C) Polarized optical microscopy images of hT crystals at RH = 0% and RH = 90%. (D) High-resolution X-ray diffraction (XRD) with a simulated parameter for projection of the orthorhombic unit cell of the hT crystal at RH = 0% and RH = 90%. (E) Summary of the conductivity enhancement of the TEMPO derivatives under applied humidity.

Conductivity Modulation of TEMPO Derivatives by Humidity Control

Building upon establishing a general conductivity trend among the TEMPO derivatives, we proceeded with a more progressive idea of enhancing or modulating the solid-state conductivity of the TEMPO derivatives. In general, TEMPO-based small molecules are expected to exhibit a crystal structure in their solid state, which minimizes the steric hindrance from the bulky substituents near the active radical. One example is that of hT in our previous work, where it showed a doubly intercalated packing structure that places the bulky substituent in an alternating manner.[23] This steric restraint among the TEMPO derivatives has been the main attribute of their failure being utilized as an effective electronic material, as the constraint inevitably accompanies considerable distancing between the active radical sites. Thus, any external stimulus that reduces the proximity between the active radical sites is expected to modulate the electronic properties of these materials significantly.

Following this idea, we repeated the solid-state conductivity measurements of the TEMPO derivatives, this time with an attached humidity controller that can reversibly and precisely control the relative humidity (RH) of the measurement system by adjusting the relative amounts of gaseous H_2O and N_2 (Figure 3). A constant voltage of 1 V was applied throughout the measurement (experimental details in the Supporting Information). Figure 3B displays the corresponding temperature-dependent conductivity of the TEMPO derivatives at RH = 90%. Interestingly, significant modulation of the conductivity was found for all of the TEMPO derivatives, at all of the temperature ranges tested. To further explore the mechanistic aspects of the observed conductivity enhancement, polarized optical microscopy (POM) and powder X-ray diffraction (pXRD) measurements were carried out for hT (Figure 3C,D). POM exhibited a distinct birefringence change that is a

https://doi.org/10.1021/jacsau.2c00361
JACS Au 2022, 2, 2089−2097

Scheme 1. Schematic Illustration Describing the Conductivity Enhancement of the TEMPO Derivatives upon Exposure to a Humid Environment and High Temperature

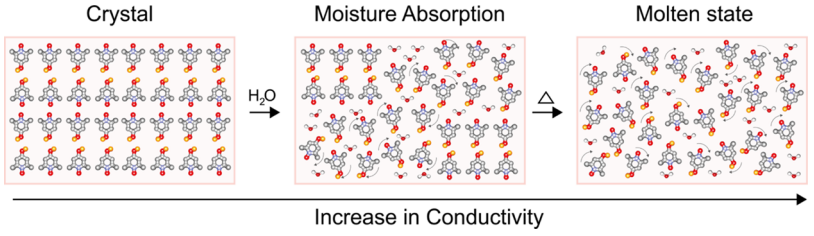

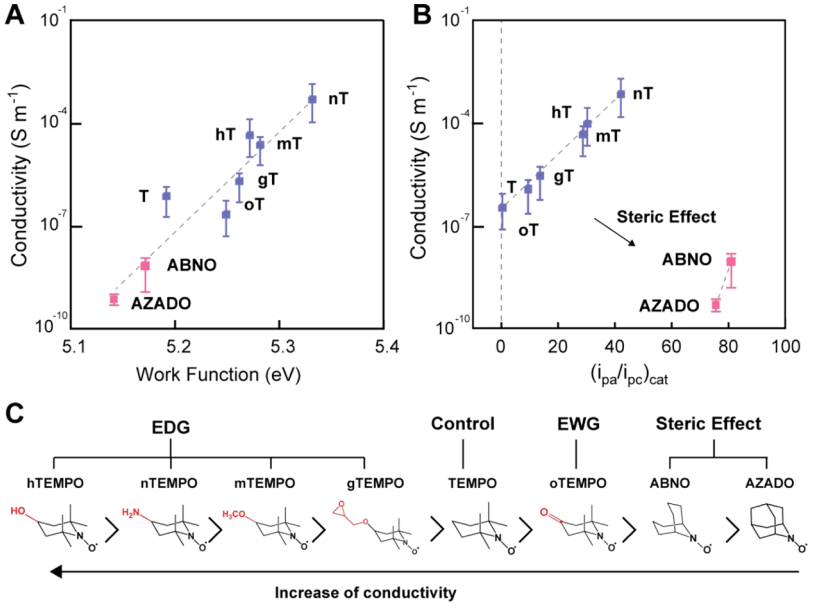

Figure 4. Structure−property−function relationship of TEMPO derivatives. (A) Plot of conductivity vs. calculated work function of selected TEMPO derivatives. The work function was converted from the absolute potential $E_a = E^\circ + 4.674$ V vs vacuum, where E° was approximated from the formal potential reported in the literature.[5] Adapted with permission from ref.[19] Copyright 2015, American Chemical Society. (B) Plot of conductivity vs. catalytic activity (I_{pa}/I_{pc}), where the activity values were extracted from a previous report.[19] 4-substituted TEMPO derivatives and sterically less hindered ones are indicated as blue and pink filled squares, respectively. (C) Structure−property relationship of TEMPO derivatives, showing a systematic increase in conductivity based on the stability of the oxoammonium cation.

characteristic of the highly crystalline form of hT at RH = 0%. In stark contrast, we found no clear birefringence change of the same sample at RH = 90%. The diffraction patterns in pXRD also corroborated this observation (Figure 3D). Specifically, we found the sharp peaks from hT at RH = 0% at 2θ = 17.1, 12.2, 21.4, and 24.6°, which correspond to (002), (111), (131), and (222) planes[23] of the crystalline hT. The intensity of these characteristic peaks decreased significantly following the exposure of hT to RH = 90%. Additionally, we tested the impact of humidity in the other TEMPO derivatives as well (XRD and DSC, Figures S10 to S14). Note the consistency found in the other derivatives. To highlight the conductivity modulation by the applied humidity, we plotted the difference in conductivity between RH at 0 and 90%, at room temperature (Figure 3E). While we found unexpected differentiation between the conductivity increases among different types of TEMPO derivatives , we generally observed a 10^1- to 10^2-fold increase in the measured conductivity. Note that we found the highest normalized delta conductivity of $\sim 10^5$ S cm^{-1} for hT.

Based on the experimental observation regarding the connection between crystallinity and conductivity found in the TEMPO derivatives, it is clear that the major mechanism that enhances the apparent conductivity under a humid environment is *via* water infiltration into the crystalline structure, which results in a partial loss of crystallinity (Scheme 1). The resulting loss of the doubly intercalated structure that once prevented effective charge transfer among TEMPO molecules enhances the proximity between active sites and facilitates conduction.[23] The unique structural feature of each TEMPO derivative then additionally determines the detailed variation of the observed conductivity. Molecular dynamics (MD) simulation on our water infiltration model for selected TEMPO derivatives (hT and T) suggests the resultant distance between the nitroxides to be ∼7 Å, which matches well with the general proximity requirements for the TEMPO-based macromolecular radical reported previously, strongly supporting our hypothesis (Figure S15).[33]

Further, we note two additional factors that affect the solid-state conductivity of TEMPO in a wet environment rather significantly: (1) the presence and/or the position of T_m, and (2) the availability of any type of secondary interaction (e.g., hydrogen bond). Specifically, while we generally find a larger increment in the observed conductivity at room temperature for the TEMPO derivatives that exhibited a characteristic crystalline structure, the increases of the amorphous ones (i.e., nT and gT) were not significant. Additionally, a large increment was also found for the one that features its T_m

https://doi.org/10.1021/jacsau.2c00361
JACS Au 2022, 2, 2089−2097

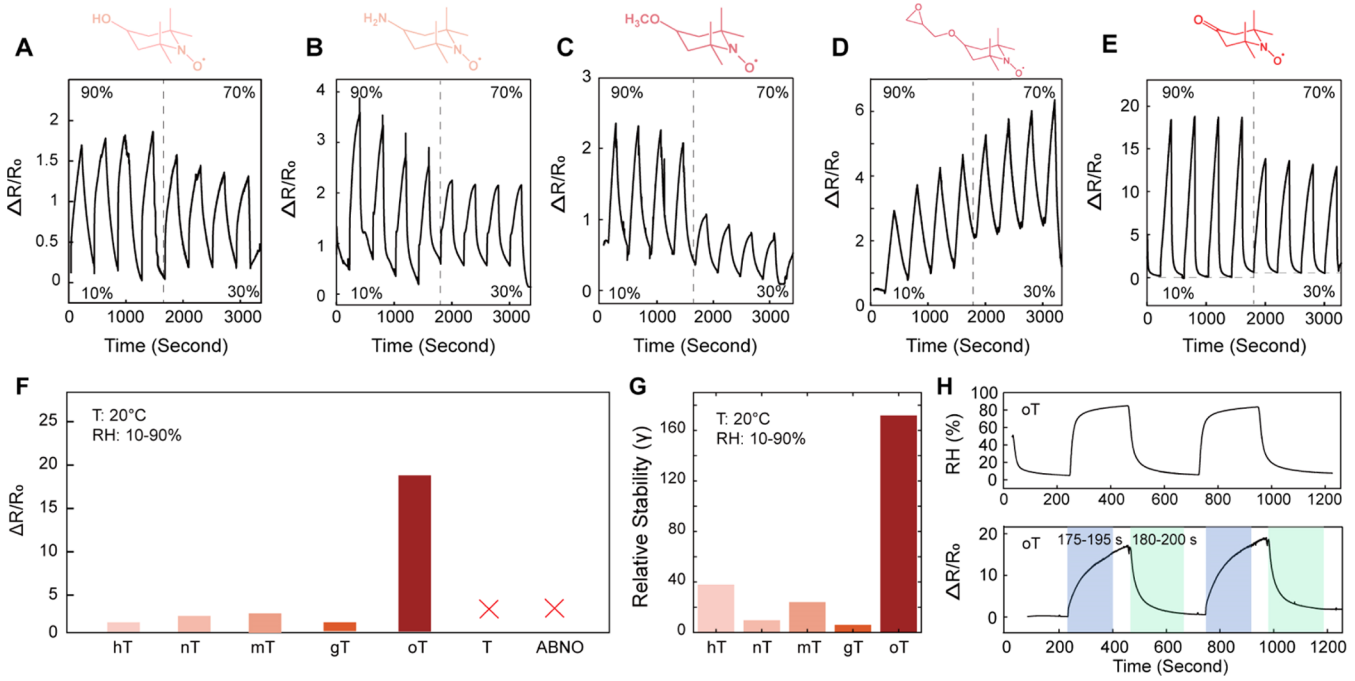

Figure 5. Humidity sensors based on TEMPO derivatives. Response curves for (A) hT, (B) nT, (C) mT, (d) gT, and (E) oT, upon the consecutive reverse RH sweep. Comparison of (F) the sensor response and (G) the device stability among the TEMPO derivatives tested. (H) Sensor characteristics of the oT device.

closer to room temperature (e.g., T). A definitive outlier was hT, which possesses both high crystallinity and the hydrogen-bonding moiety, the latter of which facilitates the infiltration of water molecules significantly. We argue this is why hT showed the largest variation in conductivity.

Our conductivity measurements reveal that solid-state conductivity under a humid environment follows the order hT> nT> mT> gT> TEMPO> oT> ABNO> AZADO as in the dry system, albeit with increased values. Overall, we note that the main purpose of this study is to provide an indirect measure of the solid-state conductivities of the TEMPO derivatives and connecting them to the trends found in their wet chemistry. The observation that the measured conductivities of the TEMPO derivatives at elevated temperature (i.e., thermally activated solid below T_m) and in a humid environment (i.e., RH = 90% at room temperature) matches with each other, and that they in turn match with their redox potential and the catalytic activity trends (*vide infra*), justifies our original hypothesis.

To gain insights into the observed solid-state conductivity trend, we sought its connection with the wet chemistry of the TEMPO derivatives that has well been established throughout the literature.[5,19] In a recent report by Hickey and co-workers, and in a separate work by Zhang and co-workers, both experimental and theoretical approaches were made on revealing the structure−function relationship of the TEMPO derivatives in a wet system.[19,22] Briefly, the redox potential of the TEMPO derivatives toward the alcohol oxidation reaction was provided, where they were utilized as catalysts. Further, these potential values were correlated with their catalytic activity, where the activity was defined as the ratio between the anodic (i_{pa}) and cathodic (i_{pc}) currents (i_{pa}/i_{pc}). Importantly, it was found that the redox potential displayed global linearity with the catalytic activities measured experimentally, showing a robust structure−function relationship governing TEMPO derivatives in a wet system. Based on these experimental findings, we hypothesized that the solid-state conductivity found in the TEMPO derivatives and the trend among them may have a similar structure−function or structure−property relationship.

Figure 4 displays the comparison of the observed solid-state conductivity of the TEMPO derivatives to the key parameters of their wet chemistry, where clear linearity between the conductivity and the redox potential (converted to the work function), as well as that with the catalytic activity, was found. Note that the comparison was made between the reported catalytic activities and the conductivities of the TEMPO derivatives at RH = 90%, both at RT. While it may seem appropriate that the measured solid-state conductivity has a linear relationship with these parameters, we find a more rigorous consideration on why it should be the case in our study is necessary. As the two parameter sets (i.e., that of solid-state conductivity and that of redox potential) are normally independent with each other in conventional (semi)-conductors, no linearity between the two is generally expected. Therefore, we attribute the observed linearity here reflects the key charge transfer mechanism of our system that is unique to the conventional ones. Specifically, it indicates that the main charge transfer mechanism in our system is the self-exchange redox reaction between the active sites of TEMPO, rather than the one being governed by the Schottky barrier and/or the Poole−Frenkel mechanism associated with the electric-field-driven mechanism, as the comparison suggests the inherent linkage between charge extraction and conduction.[5] In the latter cases (i.e., field-driven), for example, it is expected that the loss of linearity between the solid-state conductivity and the redox potential is expected as per their conceptual orthogonality, albeit the linearity between the work function and the catalytic activity remains the same, as has been reported previously.[19,22]

https://doi.org/10.1021/jacsau.2c00361
JACS Au 2022, 2, 2089−2097

In general, a nonconjugated substituent affects the oxidation potential of the TEMPO derivatives by interacting electrostatically with both the polarized bond present in the parent nitroxide (i.e., NO˙) and the formal charge formed upon its oxidation (i.e., $>N^{+}{=}O$).[22] Specifically, the orientation and the magnitude of the substituent dipole influence the electrostatic stabilization/destabilization of the oxoammonium cation, which in turn affects the oxidation potential of the parent nitroxide.[19] The observation that most of the nitroxides examined here featured the linear relationship is consistent with the notion that the electron-donating groups stabilize the oxoammonium cation (or vice versa), resulting in a lower oxidation potential and catalytic activities. It should be noted, however, that the bicyclic nitroxyl derivatives, such as ABNO and AZADO, tend to have a higher catalytic activity in an aqueous system although the geometric constraints on them generally hinder the solid-state electronic conduction.[21] This is because, unlike in conjugated systems, the charge transfer site in organic radicals is heavily localized.

To further explore the utility of the structure−property relationship of TEMPO derivatives in a more practical application, we tested their usage as active materials for a humidity sensor. Sensors based on each TEMPO derivative were fabricated similarly to the conductivity measurement system with the humidity controller, and the changes in resistance (R) were recorded and compared. For the measurement, a constant read voltage of 1 V and subsequent reverse RH sweeps from 10 to 90% were applied (experimental details in the Supporting Information). We note that the humidity sensing for all of the TEMPO derivatives tested was carried out in the RH range from 10 to 90%, due mainly to the reversibility issues. Figure 5 shows the sensor properties of the five sensors based on hT, nT, mT, gT, and oT. In general, all of the TEMPO derivatives tested showed decreasing resistance upon increasing RH, displaying a negative sensing behavior. Sensitivity, which is defined as $\Delta R/R_0$ in our experimental setup, showed a major to minor variation among different TEMPO species. For example, while the former four sensors showed sensitivity below ∼5, a notably large value of sensitivity (19.4) was found for oT (Figure 5F). For comparison, we tabulated the performance of our device with other organic material-based humidity sensors (Table S2).[34,35] Note that the sensitivity found in our device features outstanding performance, which is one of the highest among various types of humidity sensors reported in the literature based on organic materials. Furthermore, relative device stability (γ) estimated for each device showed the highest value for the oT, while the former four displayed relatively low values of γ (detailed estimation process described in the Supporting Information). This is well-reflected in their sensing behavior, where a significant level of hysteresis, inefficient adsorption/desorption of water molecules, or the baseline shifts were present among the first four. In contrast, oT showed a markedly small amount of hysteresis upon prolonged RH sweep, showing a minimal baseline shift even after repeated cycles. We further note that, while the largest change in the observed conductivity was found for hT (Figure 5), oT showed the largest humidity-sensing ability in the range tested (RH = 10% to RH = 90%) (Figure S16). We further characterized the sensor characteristics of oT based on its high performance and stability (Figure 5H). Response and recovery times, which are defined as the time required to reach 90% of the equilibrium response upon humidification/dehumidification, were measured to be 175−195 and 180−200 s, respectively. Overall, we believe the high performance of the oT-based device is based on its characteristic humidity-sensing mechanism, which is not limited to a simple adsorption−desorption of infiltrated water molecules that most other devices are based on (Figures 2 and 4). Specifically, we notice that the T_m of oT, which leads to a large variation in conductivity, occurs around room temperature at RH = 0%, the temperature at which the sensor experiments were carried out (Figure 2). Regarding the device stability of oT, we find that the oT is much less hygroscopic than the other four TEMPO derivatives tested, the nature of which should clearly affect the effective adsorption/desorption of water molecules upon exposure at a high RH value.

CONCLUSIONS

While significant research efforts have been made on the macromolecular forms of organic radicals and the wet chemistry of small-molecular radicals, solid-state organic radicals have largely been unexplored. We presented a comprehensive description of organic radicals in general by demonstrating the structure−property relationship governing the small-molecular radicals and illustrated the context they are in, in the subfields of open-shell chemistry. We believe our work can serve as an initiative in searching for different types of designer small- and macromolecular radicals, targeting exciting opportunities that future open-shell electronics present.

ASSOCIATED CONTENT

Supporting Information

The Supporting Information is available free of charge at https://pubs.acs.org/doi/10.1021/jacsau.2c00361.

Experimental section, physical properties of TEMPO derivatives, ESR and pXRD spectra, DSC thermograms, MD simulations, ultraviolet photoelectron spectroscopy (UPS), and $I-V$ curve of hT (PDF)

AUTHOR INFORMATION

Corresponding Author

Yongho Joo − *Institute of Advanced Composite Materials, Korea Institute of Science and Technology (KIST), Wanju-gun, Jeonbuk 55324, Republic of Korea;* orcid.org/0000-0002-1149-9105; Email: yjoo0727@kist.re.kr

Authors

Jaehyoung Ko − *Institute of Advanced Composite Materials, Korea Institute of Science and Technology (KIST), Wanju-gun, Jeonbuk 55324, Republic of Korea; Department of Chemical and Biomolecular Engineering and KAIST Institute for Nano Century, Korea Advanced Institute of Science and Technology (KAIST), Daejeon 34141, Republic of Korea*

Ilhwan Yu − *Institute of Advanced Composite Materials, Korea Institute of Science and Technology (KIST), Wanju-gun, Jeonbuk 55324, Republic of Korea*

Seung-Yeol Jeon − *Institute of Advanced Composite Materials, Korea Institute of Science and Technology (KIST), Wanju-gun, Jeonbuk 55324, Republic of Korea*

Daewon Sohn − *Department of Chemistry, Hanyang University, Seoul 04763, Republic of Korea;* orcid.org/0000-0002-7200-9683

Sung Gap Im − *Department of Chemical and Biomolecular Engineering and KAIST Institute for Nano Century, Korea*

https://doi.org/10.1021/jacsau.2c00361
JACS Au 2022, 2, 2089−2097

Advanced Institute of Science and Technology (KAIST), Daejeon 34141, Republic of Korea; orcid.org/0000-0002-2802-6398

Complete contact information is available at: https://pubs.acs.org/10.1021/jacsau.2c00361

Author Contributions

The manuscript was written through contributions of all authors. All authors have given approval to the final version of the manuscript. CRediT: **Jaehyoung Ko** data curation, formal analysis, investigation, validation, writing-original draft, writing-review & editing; **Ilhwan Yu** data curation, formal analysis; **Seung-Yeol Jeon** data curation, formal analysis, investigation, methodology, software; **Daewon Sohn** supervision, validation, writing-original draft; **Sung Gap Im** investigation, supervision, writing-original draft; **Yongho Joo** funding acquisition, investigation, project administration, supervision, validation, visualization, writing-original draft, writing-review & editing.

Notes

The authors declare no competing financial interest.

■ ACKNOWLEDGMENTS

The authors acknowledge useful discussion with Prof. Chang Yun Son. This work was supported by the Korea Institute of Science and Technology (KIST, Korea) Institutional Program, by the National Research Foundation of Korea (NRF) grant funded by the Korea government (MSIT) (2020R1C1C1005005 and CPS21081-100), and by the National Research Foundation of Korea (NRF) grant funded by the Korea Government (MSIT) (No.2021R1-A2B5B03001416).

■ REFERENCES

(1) Joo, Y.; Agarkar, V.; Sung, S. H.; Savoie, B. M.; Boudouris, B. W. A nonconjugated radical polymer glass with high electrical conductivity. *Science* **2018**, *359*, 1391−1395.
(2) Rostro, L.; Wong, S. H.; Boudouris, B. W. Solid state electrical conductivity of radical polymers as a function of pendant group oxidation state. *Macromolecules* **2014**, *47*, 3713−3719.
(3) Rostro, L.; Baradwaj, A. G.; Boudouris, B. W. Controlled radical polymerization and quantification of solid state electrical conductivities of macromolecules bearing pendant stable radical groups. *ACS Appl. Mater. Interfaces* **2013**, *5*, 9896−9901.
(4) Baradwaj, A. G.; Wong, S. H.; Laster, J. S.; Wingate, A. J.; Hay, M. E.; Boudouris, B. W. Impact of the addition of redox-active salts on the charge transport ability of radical polymer thin films. *Macromolecules* **2016**, *49*, 4784−4791.
(5) Oyaizu, K.; Nishide, H. Radical polymers for organic electronic devices: a radical departure from conjugated polymers? *Adv. Mater.* **2009**, *21*, 2339−2344.
(6) Yonekuta, Y.; Honda, K.; Nishide, H. A non-volatile, bistable, and rewritable memory device fabricated with poly(nitroxide radical) and silver salt layers. *Polym. Adv. Technol.* **2008**, *19*, 281−284.
(7) Yonekuta, Y.; Susuki, K.; Oyaizu, K.; Honda, K.; Nishide, H. Battery-inspired, nonvolatile, and rewritable memory architecture: a radical polymer-based organic device. *J. Am. Chem. Soc.* **2007**, *129*, 14128−14129.
(8) Zhang, Y.; Park, A. M.; McMillan, S. R.; Harmon, N. J.; Flatté, M. E.; Fuchs, G. D.; Ober, C. K. Charge Transport in Conjugated Polymers with Pendent Stable Radical Groups. *Chem. Mater.* **2018**, *30*, 4799−4807.
(9) Lutkenhaus, J. A radical advance for conducting polymers. *Science* **2018**, *359*, 1334−1335.
(10) Sato, K.; Ichinoi, R.; Mizukami, R.; Serikawa, T.; Sasaki, Y.; Lutkenhaus, J.; Nishide, H.; Oyaizu, K. Diffusion-cooperative model for charge transport by redox-active nonconjugated polymers. *J. Am. Chem. Soc.* **2018**, *140*, 1049−1056.
(11) Nakahara, K.; Oyaizu, K.; Nishide, H. Electrolyte anion-assisted charge transportation in poly (oxoammonium cation/nitroxyl radical) redox gels. *J. Mater. Chem.* **2012**, *22*, 13669−13673.
(12) Janoschka, T.; Hager, M. D.; Schubert, U. S. Powering up the future: radical polymers for battery applications. *Adv. Mater.* **2012**, *24*, 6397−6409.
(13) Nishide, H.; Suga, T. Organic radical battery. *Electrochem. Soc. Interface* **2005**, *14*, 32−38.
(14) Wang, S.; Li, F.; Easley, A. D.; Lutkenhaus, J. L. Real-time insight into the doping mechanism of redox-active organic radical polymers. *Nat. Mater.* **2019**, *18*, 69−75.
(15) Wang, S.; Easley, A. D.; Lutkenhaus, J. L. 100th Anniversary of Macromolecular Science Viewpoint: Fundamentals for the Future of Macromolecular Nitroxide Radicals. *ACS Macro Lett.* **2020**, *9*, 358−370.
(16) Oyaizu, K.; Ando, Y.; Konishi, H.; Nishide, H. Nernstian adsorbate-like bulk layer of organic radical polymers for high-density charge storage purposes. *J. Am. Chem. Soc.* **2008**, *130*, 14459−14461.
(17) Xie, Y.; Zhang, K.; Yamauchi, Y.; Oyaizu, K.; Jia, Z. Nitroxide radical polymers for emerging plastic energy storage and organic electronics: fundamentals, materials, and applications. *Mater. Horiz.* **2021**, *8*, 803−829.
(18) Nishide, H.; Oyaizu, K. Toward flexible batteries. *Science* **2008**, *319*, 737−738.
(19) Hickey, D. P.; Schiedler, D. A.; Matanovic, I.; Doan, P. V.; Atanassov, P.; Minteer, S. D.; Sigman, M. S. Predicting Electrocatalytic Properties: Modeling Structure−Activity Relationships of Nitroxyl Radicals. *J. Am. Chem. Soc.* **2015**, *137*, 16179−16186.
(20) Nutting, J. E.; Rafiee, M.; Stahl, S. S. Tetramethylpiperidine N-Oxyl (TEMPO), Phthalimide N-Oxyl (PINO), and Related N-Oxyl Species: Electrochemical Properties and Their Use in Electrocatalytic Reactions. *Chem. Rev.* **2018**, *118*, 4834−4885.
(21) Rafiee, M.; Miles, K. C.; Stahl, S. S. Electrocatalytic Alcohol Oxidation with TEMPO and Bicyclic Nitroxyl Derivatives: Driving Force Trumps Steric Effects. *J. Am. Chem. Soc.* **2015**, *137*, 14751−14757.
(22) Zhang, K.; Noble, B. B.; Mater, A. C.; Monteiro, M. J.; Coote, M. L.; Jia, Z. Effect of heteroatom and functionality substitution on the oxidation potential of cyclic nitroxide radicals: role of electrostatics in electrochemistry. *Phys. Chem. Chem. Phys.* **2018**, *20*, 2606−2614.
(23) Yu, I.; Jo, Y.; Ko, J.; Kim, D.-Y.; Sohn, D.; Joo, Y. Making Nonconjugated Small-Molecule Organic Radicals Conduct. *Nano Lett.* **2020**, *20*, 5376−5382.
(24) Bhat, G. A.; Rashad, A. Z.; Ji, X.; Quiroz, M.; Fang, L.; Darensbourg, D. J. TEMPO Containing Radical Polymonothiocarbonate Polymers with Regio- and Stereo-Regularities: Synthesis, Characterization, and Electrical Conductivity Studies. *Angew. Chem., Int. Ed.* **2021**, *60*, 20734−20738.
(25) Tan, Y.; Casetti, N. C.; Boudouris, B. W.; Savoie, B. M. Molecular Design Features for Charge Transport in Nonconjugated Radical Polymers. *J. Am. Chem. Soc.* **2021**, *143*, 11994−12002.
(26) Chung, J.; Khot, A.; Savoie, B. M.; Boudouris, B. W. 100th Anniversary of Macromolecular Science Viewpoint: Recent Advances and Opportunities for Mixed Ion and Charge Conducting Polymers. *ACS Macro Lett.* **2020**, *9*, 646−655.
(27) Joo, Y.; Mukherjee, S.; Boudouris, B. W. Radical Polymers Alter the Carrier Properties of Semiconducting Carbon Nanotubes. *ACS Appl. Polym. Mater.* **2019**, *1*, 204−210.
(28) Ponder, J. F.; Gregory, S. A.; Atassi, A.; Menon, A. K.; Lang, A. W.; Savagian, L. R.; Reynolds, J. R.; Yee, S. K. Significant Enhancement of the Electrical Conductivity of Conjugated Polymers by Post-Processing Side Chain Removal. *J. Am. Chem. Soc.* **2022**, *144*, 1351−1360.

(29) Jo, Y.; Yu, I.; Ko, J.; Kwon, J. E.; Joo, Y. Sequential Codoping Making Nonconjugated Organic Radicals Conduct Ionically Electronically. *Small Sci.* **2022**, *2*, No. 2100081.
(30) Tomlinson, E. P.; Hay, M. E.; Boudouris, B. W. Radical polymers and their application to organic electronic devices. *Macromolecules* **2014**, *47*, 6145−6158.
(31) Suga, T.; Pu, Y.-J.; Oyaizu, K.; Nishide, H. Electron-transfer kinetics of nitroxide radicals as an electrode-active material. *Bull. Chem. Soc. Jpn.* **2004**, *77*, 2203−2204.
(32) Nishide, H.; Iwasa, S.; Pu, Y.-J.; Suga, T.; Nakahara, K.; Satoh, M. Organic radical battery: nitroxide polymers as a cathode-active material. *Electrochim. Acta* **2004**, *50*, 827−831.
(33) Kemper, T. W.; Larsen, R. E.; Gennett, T. Density of States and the Role of Energetic Disorder in Charge Transport in an Organic Radical Polymer in the Solid State. *J. Phys. Chem. C* **2015**, *119*, 21369−21375.
(34) Zhu, P.; Ou, H.; Kuang, Y.; Hao, L.; Diao, J.; Chen, G. Cellulose Nanofiber/Carbon Nanotube Dual Network-Enabled Humidity Sensor with High Sensitivity and Durability. *ACS Appl. Mater. Interfaces* **2020**, *12*, 33229−33238.
(35) Duan, Z.; Jiang, Y.; Zhao, Q.; Huang, Q.; Wang, S.; Zhang, Y.; Wu, Y.; Liu, B.; Zhen, Y.; Tai, H. Daily writing carbon ink: Novel application on humidity sensor with wide detection range, low detection limit and high detection resolution. *Sens. Actuators B: Chem.* **2021**, *339*, No. 129884.

https://doi.org/10.1021/jacsau.2c00361
JACS Au 2022, 2, 2089−2097